FINITE ELEMENT SIMULATION OF LEAKY SURFACE WAVE PROPAGATION EXCITED BY A LINE-FOCUSED TRANSDUCER

Koichiro Kawashima, Toshihiro Ito and Kiichiro Mori

Department of Mechanical Engineering
Nagaya Institute of Technology
Nagoya 466, Japan

INTRODUCTION

The use of a PVDF line-focused ultrasonic transducer with a large aperture makes possible to measure the velocities of the leaky Rayleigh, surface SV and creeping waves in time domain [1-3]. The velocities and attenuation of these waves are affected by deviation from the perfect plane, namely surface roughness, waviness, etc. They also depend on the subsurface structure. Theoretical analyses of wave propagation are possible for simple geometries and subsurface structures, however, numerical analyses of wave motion are necessary to solve many real problems. The finite element modeling of ultrasonic wave propagation has been applied for solids [4-6] and for the axisymmetric solid/fluid interface [7]. This paper gives a finite element simulation of plane leaky surface wave propagation at the solid/liquid interface excited by a line-focused transducer.

FINITE ELEMENT MODELING

A two dimensional model to be analyzed is shown in Fig.1. At the cylindrical surface, an acceleration pulse is given. The couplant water is filled on the aluminum block, of which side and bottom is free surface. The shaded side is rigid wall. Plane strain is assumed in the direction z.

In the liquid, the governing equation for pressure is given by

$$\nabla^2 p - \frac{1}{c^2}\ddot{p} = 0 \tag{1}$$

$$c = \sqrt{K / \rho_\ell} \tag{2}$$

where p is pressure, K and ρ_ℓ are the bulk modulus and density of the liquid.

The governing equations for an isotropic solid are given by

Review of Progress in Quantitative Nondestructive Evaluation, Vol 17
Edited by D.O. Thompson and D.E. Chimenti, Plenum Press, New York, 1998

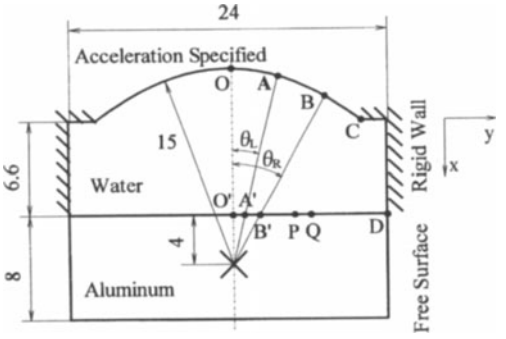

Figure 1. Geometric dimensions of the analyzed field.

$$\frac{\partial \sigma_{ij}}{\partial x_j} = \rho_s \ddot{u}_i \tag{3}$$

where σ_{ij} is stress, ρ_s is the density of the solid and $\ddot{u}_i$ is particle acceleration.

At the solid/liquid interface, the pressure, acceleration and stress are related by the following relations

$$\frac{\partial p}{\partial \mathbf{n}} = -\rho_\ell \ddot{\mathbf{u}}_n \qquad \text{(at acceleration specified surface)} \tag{4}$$

$$\sigma_{ij} n_j = -p n_i \qquad \text{(at solid/liquid interface)} \tag{5}$$

where $\mathbf{n}$ is the unit normal to the boundary and $\mathbf{u}_n$ is the displacement in that direction.

The governing equations of a finite element are derived with the method of weighted residuals [8].

$$[H]\{p\} + [G]\{\ddot{p}\} + [L]\{\ddot{w}_s\} + \{F\} = \{0\} \tag{6}$$

$$[M]\{\ddot{u}\} + [K]\{u\} = [\ell]\{p\} \tag{7}$$

$$H_{ij} = \frac{1}{c^2}\int_V \left(\frac{\partial N_i}{\partial x}\frac{\partial N_j}{\partial x} - \frac{\partial N_i}{\partial y}\frac{\partial N_j}{\partial y}\right) dV, \quad G_{ij} = \frac{1}{c^2}\int_V N_i N_j dV,$$

$$L_{ij} = \rho_\ell \int_{\Gamma s/\ell} N_i N_j dS, \quad F_i = \rho_\ell \int_{\Gamma a} N_i \ddot{\mathbf{u}}_n dS,$$

$$M_{ij} = \rho_s \int_V N_i N_j dV, \quad K_{ij} = \int_V B_{ir}^T D_{rs} B_{sj} dV, \quad \ell_{ij} = \int_{\Gamma s/\ell} N_i N_j dS \tag{8}$$

where N is a shape function, B is a strain shape function and D is the elasticity matrix for plane strain. Γ_a denotes the boundary with specified acceleration and $\Gamma_{s/\ell}$ is the solid/fluid interface.

For time integration by the Runge-Kutta method, equations (6) and (7) are expressed

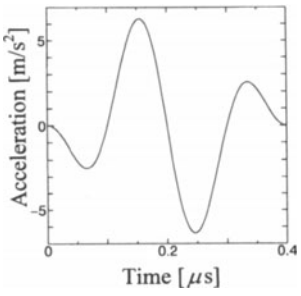

Figure 2. The acceleration profile of the input wave.

in the following forms

$$\{\frac{du}{dt}\} = \{\dot{u}\} \tag{9}$$

$$\{\frac{dp}{dt}\} = \{\dot{p}\} \tag{10}$$

$$\{\frac{d\dot{u}}{dt}\} = -[M]^{-1}([K]\{u\} - [\ell]\{p\}) \tag{11}$$

$$\{\frac{d\dot{p}}{dt}\} = -[G]^{-1}\langle[H]\{p\} - [L]\{[M]^{-1}([K]\{u\} - [\ell]\{p\})\} + \{F\}\rangle . \tag{12}$$

NUMERICAL CALCULATION AND RESULTS

Fluid and solid in Fig.1 are assumed to be water and 2017 aluminum alloy. They are discretized by linear triangular elements. For satisfying the stability condition, the integration time step Δt and element size h are restricted by

$$h \le 0.06\lambda \tag{13}$$

$$\Delta t \le 0.3h / V_l \tag{14}$$

where λ and V_l are the wavelength and velocity of the longitudinal wave in the solid. The following material constants are assumed:

$K = 2.195$GPa, $\rho_\ell = 998.3$kg/m^3 for water;

$E = 71.5$GPa, $\nu = 0.339$, $\rho_s = 2700$kg/m^3 for 2017 aluminum.

The cylindrical surface of a focal length 15mm is exited by the acceleration pulse of 5MHz shown in Fig.2

Wave Profile

In the following, figures (a) show the pressure profiles in the water, and in figures (b) the displacement component normal to the solid/fluid interface is drawn. In each figure, t denotes the time elapsed after launching a pulse on the cylindrical surface. In Figs. 4, 6

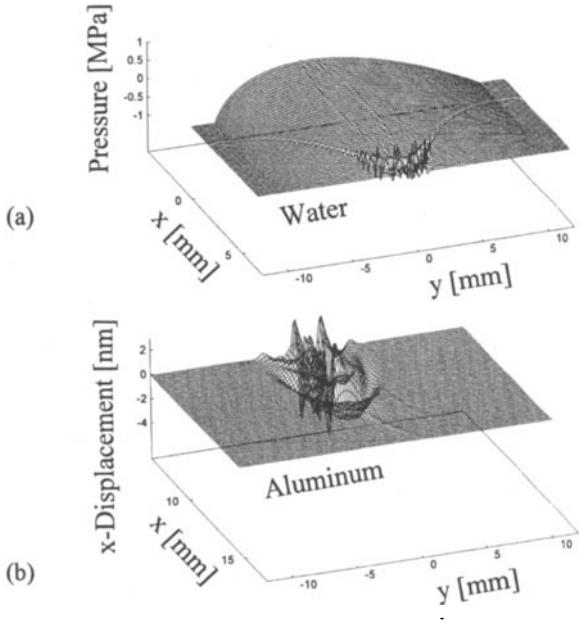

Figure 3. Wave profiles in water and aluminum ($t = 8\mu s$).

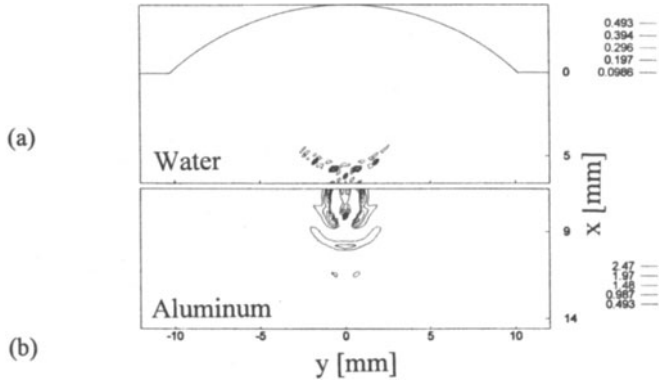

Figure 4. Wave profiles in water and aluminum ($t = 8\mu s$).

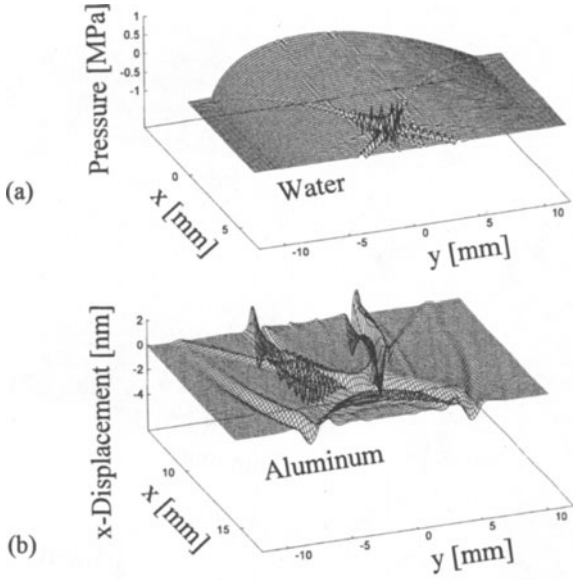

Figure 5. Wave profiles in water and aluminum ($t = 9\mu$s).

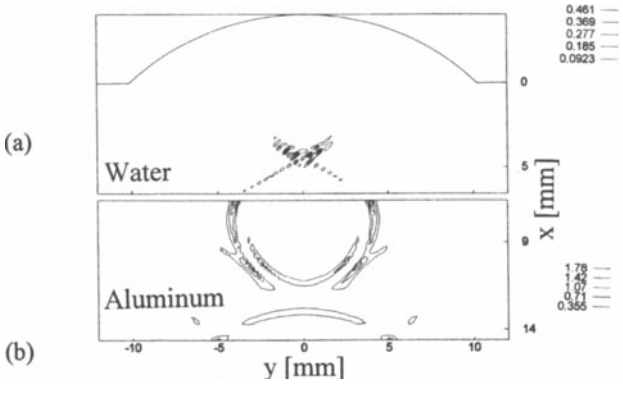

Figure 6. Wave profiles in water and aluminum ($t = 9\mu$s).

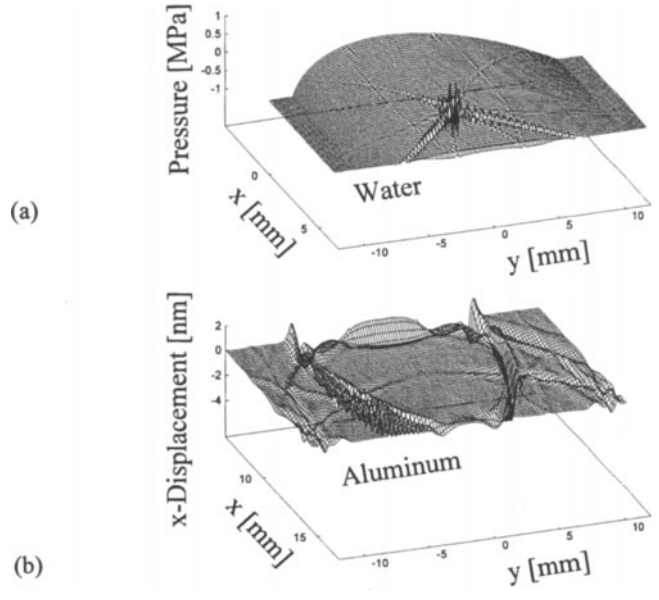

Figure 7. Wave profiles in water and aluminum ($t = 10\mu$ s).

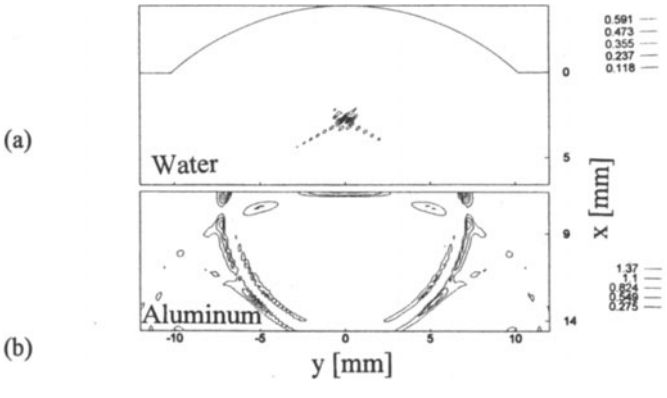

Figure 8. Wave profiles in water and aluminum ($t = 10\mu$ s).

and 8, the contours of the pressure and displacement are plotted to illustrate wavefronts.

Main events, which are not shown in the following figures, in the wave propagation process are as follows: At $t = 4.9\mu$s the wave emitted from C in Fig.1 reaches the corner D, from which wave propagates through water and aluminum. Thus, two semi-circular wave fronts appear in the water as shown in Figs. 3(a), 5(a) and 7(a). At $t = 7\mu$s the wave propagated along the path BB' in Fig.1 reaches the aluminum surface and the leaky Rayleigh wave with large amplitude is excited. Similarly, at $t = 7.3\mu$s the creeping wave is excited on the aluminum surface by the wave traveled along AA'. At $t = 7.4\mu$s the wave along the symmetric axis hits the point O' and the bulk waves propagate through the aluminum. Of course, the longitudinal wave travel back in the water.

The wave profiles shown in Figs. 3(b) and 4(b) depict clearly the leaky Rayleigh wave at the water/aluminum interface and the longitudinal and transverse waves in the aluminum. In Fig. 5(b), we see the longitudinal, transverse and head waves. A part of the longitudinal wave front is reflected at the bottom of the aluminum block. At the water/aluminum interface, it is clearly shown that the Rayleigh wave ($y = \pm 4$ mm) of large amplitude as well as the creeping wave ($y = \pm 9$ mm). In the water, the corresponding leaky waves are seen in Figs. 5(a) and 6(a). The inclinations of these leaky wavefronts to the water/aluminum interface are 14° for the creeping wave and 30° for the leaky Rayleigh wave, which are very close to the critical angle of the longitudinal and transverse waves. In Fig. 7(b), the longitudinal wave reflected at the bottom reaches the water/aluminum interface and the transverse wave reaches the bottom surface. The mode-converted transverse wave from the longitudinal wave is also noticed.

Velocities of the leaky Rayleigh and creeping waves

The temporal variation of the normal displacement to the water/aluminum interface is shown in Fig. 9 for the point P and Q in Fig.1, which are away 5 and 6 mm from the center O'. The right end wavelet and the next are the leaky Rayleigh and creeping waves, respectively. The velocities of these waves have been calculated and shown in Table I with the measured ones. For the leaky Rayleigh wave, the finite element simulation is very close to the experimental result. However, the agreement of the creeping wave velocity is not so good, because of small amplitude.

CONCLUSION

The ultrasonic wave propagation excited by a line-focus transducer has been analyzed by finite element method for water and an aluminum block. The leaky Rayleigh and creeping waves on the water/aluminum interface are simulated well. The waves leaked from these waves into water also have been simulated. The calculated velocities of the leaky Rayleigh and creeping waves are 2967 and 6263m/s, which are close to the measured ones.

Table I. The velocities of the surface waves.

	Numerical simulation	Experimental	Error
Leaky Rayleigh wave	2967 m/s	2943 m/s	+0.8 %
Creeping wave	6263 m/s	6350 m/s	-1.4 %

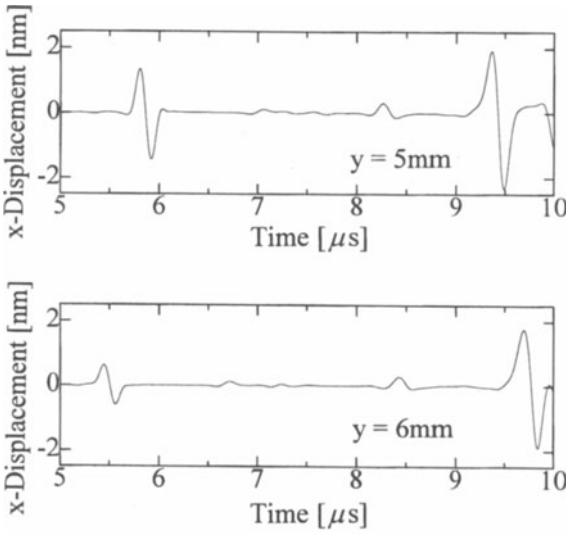

Figure 9. The variation of the x-displacements at point P and Q.

REFERENCES

1. D.Xiang, N.N.Hsu and G.V.Blessing, in *Review of Progress in QNDE*, Vol.15, eds. D.O.Thompson and D.E.Chimenti (Plenum, New York, 1996), p.1431.
2. G.Gondard, F.Tady, MH.Noroy, L.Paradis and JC.Baboux, in *Review of Progress in QNDE*, Vol.15, *op. cit.* (1996), p.1605.
3. I.Fujii, K.Kawashima and T.Sato, Trans. JSME Ser.A, 63, 2444 (1997).
4. R.Ludwig and W.Load, IEEE Trans. UFFC, 35, 809 (1988).
5. W.Load, R.Ludwig and Z.You, J. NDE, 9, 129 (1990).
6. Z.You, M.Lust. R.Ludwig and W.Load, IEEE Trans. UFFC, 38, 436 (1991).
7. T.Xue, W.Lord, S.Udpa, L.Udpa and M.Mina, in *Review of Progress in QNDE*, Vol.15, *op. cit.* (1996), p.299.
8. T.Tsuta, S.Okamoto and S.Yokoi, Trans. JSME Ser.C, 60, 1917 (1994).